SLAC-PUB-9744

The B System as a Window to New Physics

Presented at 3rd International Conference on B Physics and CP Violation
(BCONF99), 12/3/1999—12/7/1999, Taipei, Taiwan

Stanford Linear Accelerator Center, Stanford University, Stanford, CA 94309

Work supported by Department of Energy contract DE–AC03–76SF00515.

THE B SYSTEM AS A WINDOW TO NEW PHYSICS

J.L. HEWETT
Stanford Linear Accelerator Center, Stanford CA 94309, USA

The opportunities to explore physics beyond the Standard Model in the B meson system are described. After denoting some overall features which are generic consequences of the search for new physics, we concentrate on the effects of new interactions in flavor changing neutral current transitions, focusing on supersymmetry and the left-right symmetric model as specific examples of new physics scenarios.

1 Overview

The B-meson system promises to yield a fertile testing ground of the Standard Model (SM). With the impressive start-up of the SLAC and KEK B-Factories, as well as the large data samples which will be acquired over the next decade at CESR, the Tevatron, and the LHC, the SM willed be probed at an unprecedented level of precision. It is well-known that precision measurements of low-energy processes can provide insight to very high energy scales via the indirect effects of new interactions. As such, the B sector offers a complementary probe of new physics, and in some cases may yield constraints which surpass those from direct collider searches or exclude entire classes of models.

The existence of new physics may modify the low-energy effective Hamiltonian governing B decays by (i) giving new contributions to the SM operators, (ii) generating new operators, or (iii) with the presence of new CP violating phases. In fact, calculations [1] of electroweak baryogenesis within the SM show that the produced baryon asymmetry is too small by many orders of magnitude and hence suggests that new CP violating phases must exist in nature. However, new physics cannot change properties that we know to be true, such as $a_{CP}(\psi K_s) = -a_{CP}(\psi K_L)$, and is unlikely to compete in processes which receive large SM contributions, such as $B(b \to c\bar{u}d)$.

The best way to probe for new physics is to employ observables which are easy to measure, have small SM uncertainties, and are likely to be sensitive to new interactions. New physics may manifest itself in the B system in several ways, for example, inconsistencies with the SM may be found between precision measurements of the sides and angles of the unitarity triangle, in rare decays, in B meson mixing, or in processes which are predicted to vanish in the SM. In particular, one would expect large effects from new interactions in 1-loop processes or in observables which are suppressed in the SM. Processes which provide good examples of the latter scenario are the CP asymmetries in $B_s \to \psi\phi$ and $B_s \to D_s^+ D_s^-$, the direct CP asymmetries in $B^\pm \to \psi K^\pm$ and $b \to$

$s\gamma$, the semi-leptonic asymmetry in $B_{d,s}$ mixing, and $D - \bar{D}$ mixing. It is anticipated that additional tree-level contributions to B decay are suppressed, since the scale of new physics is expected to be large compared to M_W,

Here, we concentrate on the loop effects of new interactions in flavor changing neutral current (FCNC) transitions. We note that most classes of models which induce large effects in the FCNC decays also affect $B_d^0 - \bar{B}_d^0$ mixing, and that measurements of several different loop-level processes may elucidate the origin of new interactions. In addition, long distance effects are expected to play less of a role due to the heavy B mass, and hence rare processes are essentially short distance dominated.

2 New Physics Constraints from $B_d - \bar{B}_d$ Mixing

Constraints on the magnitude and phase of potential new physics contributions to $B_d - \bar{B}_d$ mixing can be obtained[2] from the recent CDF measurement[3] of the CP asymmetry in $B \to \psi K_S$ decays. This measurement yields a value for the unitarity triangle $\sin 2\beta$ from an interference of the phases in the amplitudes for B_d mixing and tree-level decay. Assuming that the 3×3 CKM matrix is unitary and that the tree-level decay, in particular its phase, is dominated by SM contributions, the new physics effects in B_d mixing can then be isolated. The modification to the magnitude and phase of the B_d mixing amplitude, M_{12}, can be expressed in a model independent fashion by

$$M_{12} = r_d^2 e^{2i\theta_d} M_{12}^{SM} \,. \tag{1}$$

The direct measurement of Δm_B provides bounds on the magnitude of new physics contributions, r_d, while the CDF results constrains new phases, θ_d. Taking into account the uncertainties on the values of the relevant CKM angles and hadronic matrix elements, Barenboim *et al.*[2] find

$$0.3 \lesssim r_d^2 \lesssim 5 \,, \tag{2}$$

and

$$\sin 2\theta_d \gtrsim -0.6\,(-0.87) \,, \tag{3}$$

at 1σ (95% C.L.). It is clear that large contributions to this process from new interactions are still allowed, and may hence admit for an exciting discovery as future measurements improve.

3 Formalism for $b \to s$ Transitions

The observation[4] of radiative penguin mediated processes, in both the exclusive $B \to K^*\gamma$ and inclusive $B \to X_s\gamma$ channels, has placed the study of rare B

decays on a new footing and has provided powerful constraints on classes of models.

The effective field theory for $b \to s$ transitions is summarized at this meeting by Misiak and Morozumi;[5] however, we briefly review the features which are essential to the remainder of this talk. Incorporating QCD corrections, these transitions are governed by the Hamiltonian

$$\mathcal{H}_{eff} = \frac{-4G_F}{\sqrt{2}} V_{tb} V_{ts}^* \sum_{i=1}^{10} C_i(\mu) \mathcal{O}_i(\mu) \,, \tag{4}$$

where the $\mathcal{O}_i$ are a complete set of renormalized operators of dimension six or less which mediate these transitions. The C_i represent the corresponding Wilson coefficients which are evaluated perturbatively at the electroweak scale, where the matching conditions are imposed, and then evolved down to the renormalization scale $\mu \approx m_b$. The expressions for $C_i(M_W)$ at the electroweak scale in the SM are given by the Inami-Lim functions.[6]

3.1 $B \to X_s \ell^+ \ell^-$ in the Standard Model

For $B \to X_s \ell^+ \ell^-$ this formalism leads to the physical decay amplitude (neglecting m_s and m_ℓ)

$$\begin{aligned} \mathcal{M} \;\; = \;\; & \frac{\sqrt{2} G_F \alpha}{\pi} V_{tb} V_{ts}^* \Big[C_9^{eff} \bar{s}_L \gamma_\mu b_L \bar{\ell} \gamma^\mu \ell + C_{10} \bar{s}_L \gamma_\mu b_L \bar{\ell} \gamma^\mu \gamma_5 \ell \\ & - 2 C_7^{eff} m_b \bar{s}_L i \sigma_{\mu\nu} \frac{q^\nu}{q^2} b_R \bar{\ell} \gamma^\mu \ell \Big] \,, \end{aligned} \tag{5}$$

where q^2 represents the momentum transferred to the lepton pair. The next-to-leading order (NLO) analysis for this decay has been performed in Buras *et al.*[7] The $1/m_b^2$ and $1/m_c^2$ heavy quark corrections have been computed and are found to be small.[8] The resulting inclusive branching fractions are found to be $(6.25^{+1.04}_{-0.93}) \times 10^{-6}$, $(5.73^{+0.75}_{-0.78}) \times 10^{-6}$, and $(3.24^{+0.44}_{-0.54}) \times 10^{-7}$ for $\ell = e, \mu$, and τ, respectively.

3.2 $B \to X_s \gamma$ in the Standard Model

The basis for the decay $B \to X_s \gamma$ contains the first eight operators in the effective Hamiltonian of Eq. (4). The next-to-leading order logarithmic QCD corrections have been computed, leading to a much reduced renormalization scale dependence in the branching fraction. The higher-order QCD calculation involves several steps, requiring corrections to both C_7 and the matrix element

of $\mathcal{O}_7$. In addition, the 2-loop electroweak corrections have also been computed [9] and are found to slightly reduce the branching fraction. The numerical value of the branching fraction is then found to be (again, scaling to semi-leptonic decay)

$$B(B \to X_s\gamma) = (3.28 \pm 0.30) \times 10^{-4}\,. \tag{6}$$

This is well within the range observed by CLEO and ALEPH[4] which is $B = (3.15 \pm 0.35 \pm 0.41) \times 10^{-4}$ and $B = (3.38 \pm 0.74 \pm 0.85) \times 10^{-4}$, respectively, with the 95% C.L. bounds of $2 \times 10^{-4} < B(B \to X_s\gamma) < 4.5 \times 10^{-4}$. The inclusive decays are measured by analyzing the photon energy spectrum, which has been found to retain its SM predicted shape, but not necessarily its normalization, in the presence of new physics.[10]

4 Model Independent Tests for New Physics in $b \to s$ Transitions

Measurements of $B(B \to X_s\gamma)$ constrain the magnitude, but not the sign, of $C_7(\mu)$. The coefficients at the matching scale ($\mu = M_W$) can be written in the form $C_i(M_W) = C_i^{SM}(M_W) + C_i^{new}(M_W)$, where $C_i^{new}(M_W)$ represents the contributions from new interactions. Due to operator mixing, $B \to X_s\gamma$ then limits the possible values for $C_i^{new}(M_W)$ for $i = 7, 8$. These bounds are summarized in Fig. 1. Here, the solid bands correspond to the constraints obtained from the current CLEO measurement, taking into account the variation of the renormalization scale $m_b/2 \le \mu \le 2m_b$, as well as the allowed ranges of the other input parameters. The dashed bands represent the constraints when the scale is fixed to $\mu = m_b$. We note that large values of $C_8^{new}(M_W)$ (which would yield an anomalous rate for $b \to sg$) are allowed even in the region where $C_7^{new}(M_W) \simeq 0$.

Measurement of the kinematic distributions[11,12] associated with the final state lepton pair in $B \to X_s\ell^+\ell^-$ as well as the rate for $B \to X_s\gamma$ allows the determination of the sign and magnitude of all the Wilson coefficients for the contributing operators in a model independent fashion. We have performed a Monte Carlo analysis in order to ascertain how much quantitative information will be obtainable at future B-Factories and follow the procedure outlined in Ref. [13]. For the process $B \to X_s\ell^+\ell^-$, we consider the lepton pair invariant mass distribution and forward-backward asymmetry[11] for $\ell = e, \mu, \tau$, and the tau polarization asymmetry[12] for $B \to X_s\tau^+\tau^-$. A three dimensional χ^2 fit to the coefficients $C_{7,9,10}(\mu)$ is performed for three values of integrated luminosity, 3×10^7, 10^8, and 5×10^8 $B\bar{B}$ pairs, corresponding to the expected e^+e^- B-Factory luminosities of one year at design, one year at an upgraded accelerator, and the total accumulated luminosity at the end of these programs. The 95% C.L. allowed regions (including statistical errors only for $B \to X_s\ell^+\ell^-$ and a

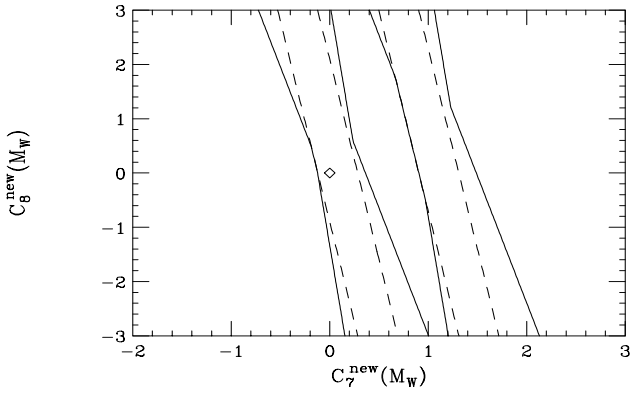

Figure 1: Bounds on the contributions from new physics to $C_{7,8}$. The region allowed by the CLEO data corresponds to the area inside the solid diagonal bands. The dashed bands represent the constraints when the renormalization scale is set to $\mu = m_b$. The diamond at the position (0,0) represents the Standard Model.

flat 10% error on $B \to X_s\gamma$) as projected onto the $C_9(\mu) - C_{10}(\mu)$ and $C_7(\mu) - C_{10}(\mu)$ planes are depicted in Figs. 2(a-b), where the diamond represents the central value for the expectations in the SM. We see that the determinations are relatively poor for 3×10^7 $B\bar{B}$ pairs and that higher statistics are required in order to focus on regions centered around the SM.

The presence of new physics may be probed via this global fit by discovering that either the values of the Wilson coefficients are altered from their SM predictions, or by obtaining a poor χ^2 for the fit, indicating that the operator basis must be extended.

5 Supersymmetric Effects in $b \to s$ Transitions

These model independent bounds can be compared with model dependent predictions for the Wilson coefficients in order to ascertain at what level specific new interactions can be probed. First, we consider supersymmetric extensions to the SM. Supersymmetry (SUSY) contains many potential sources for flavor violation. The spectroscopy of the supersymmetric states is quite model dependent and we analyze two possibilities. The first is the familiar minimal supergravity model; in this instance all the supersymmetric states follow from a common scalar mass and a common gaugino mass at the high scale. The second case is where the condition of common scalar masses is relaxed and they are allowed to take on uncorrelated values at the low scale while still preserving gauge invariance.

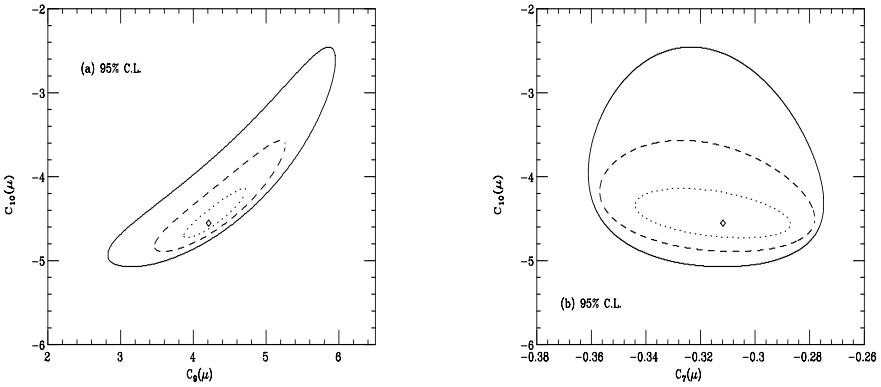

Figure 2: The 95% C.L. projections in the (a) $C_9 - C_{10}$ and (b) $C_7 - C_{10}$ planes, where the allowed regions lie inside of the contours. The solid, dashed, and dotted contours correspond to 3×10^7, 10^8, and 5×10^8 $B\bar{B}$ pairs. The central value of the SM prediction is labeled by the diamond.

We analyze the supersymmetric contributions to the Wilson coefficients [13] in terms of the quantities

$$R_i \equiv \frac{C_i^{susy}(M_W)}{C_i^{SM}(M_W)} - 1 \equiv \frac{C_i^{new}(M_W)}{C_i^{SM}(M_W)}\,, \tag{7}$$

where $C_i^{susy}(M_W)$ includes the full SM plus superpartner contributions. R_i is meant to indicate the fractional deviation from the SM value. We explore the full parameter space of the minimal supergravity model, calculate the R_i for each generated point in the supersymmetric parameter space, and then compare with the expected ability of B Factories to measure the R_i as determined by our global fit to the Wilson coefficients. Each supersymmetric solution is kept only if it is not in violation of present constraints from LEP II and Tevatron direct sparticle production limits. Our results are shown in the scatter plots of Fig. 3 in the (a) $R_7 - R_8$ and (b) $R_9 - R_{10}$ planes. The diagonal bands represent the bounds on the Wilson coefficients as previously determined from our global fit. We see from Fig. 3(a) that the current CLEO data on $B \to X_s\gamma$ already place signigicant restrictions on the supersymmetric parameter space, whereas the minimal supergravity contributions to $R_{9,10}$ are predicted to be essentially unobservable.

A second, more phenomenological approach is now adopted. The maximal

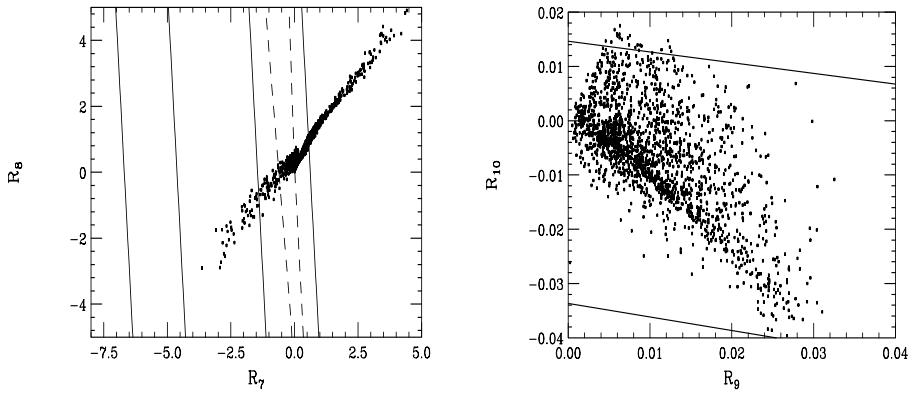

Figure 3: (a) Parameter space scatter plot of R_7 vs. R_8 in the minimal supergravity model. The allowed region from CLEO data lies inside the solid diagonal bands. The dashed band represents the potential future 10% measurement of $B \to X_s\gamma$ as described in the text. (b) Parameter space scatter plot of R_9 vs. R_{10}. The global fit to the coefficients obtained with 5×10^8 $B\bar{B}$ pairs corresponds to the region inside the diagonal bands.

effects for the parameters R_i can be estimated for a superparticle spectrum, independent of the high scale assumptions. The most important features which result in large contributions are a light $\tilde{t}_1$ state present in the SUSY spectrum and at least one light chargino state. For the dipole moment operators a light Higgsino state is also important. A pure higgsino and/or pure gaugino state have less of an effect than two mixed states when searching for maximal effects in R_9 and R_{10}. Fig. 4 displays the maximum contribution to $R_{9,10}$ versus an applicable SUSY mass scale. The other sparticle masses which are not shown ($\tilde{t}_i$, $\tilde{l}_L$, etc.) are chosen to be just above the reach of LEP II or the Tevatron, whichever yields the best bound. We see that the maximum size of $R_{9,10}$ is somewhat larger than what was allowed in the minimal supergravity model, due to the lifted restriction on mass correlations.

Given the sensitivity of the observables it is instructive to narrow our focus to the coefficient of the magnetic dipole operator. The first case we examine is that where the lightest chargino is a pure Higgsino and the lightest stop is purely right-handed: $\chi_1^\pm \sim \tilde{H}^\pm$, $\tilde{t}_1 \sim \tilde{t}_R$. The resulting contribution to R_7 is shown as a function of the $\tilde{t}_R$ mass in Fig. 5 (dashed line) for the case of $m_{\chi_1^\pm} \gtrsim M_W$. Note that the SUSY contribution to $C_7(M_W)$ in this limit always adds constructively to that of the SM. Next we examine the limit where the light chargino is a pure Wino, this contribution is shown in Fig. 5 (dotted line). Our third limiting case is that of a highly mixed $\tilde{t}_1$ state. We find

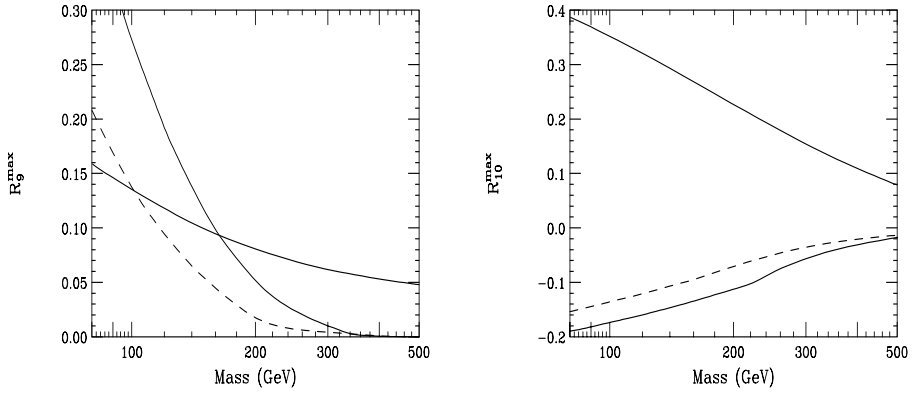

Figure 4: The maximum value of (a) R_9 and (b) R_{10} achievable for general supersymmetric models. The top solid line comes from the $t - H^{\pm}$ contribution and is displayed versus the $H^{\pm}$ mass. The bottom solid line is from the $\tilde{t}_i - \chi_j^{\pm}$ contribution with $\tan\beta = 1$ and is shown versus the $\chi_i^{\pm}$ mass. The dashed line is the $\tilde{t}_i - \chi_j^{\pm}$ contribution with $\tan\beta = 2$. The other mass parameters which are not plotted are chosen to be just above the reach of LEP II and the Tevatron.

that in this case large $\tan\beta$ solutions ($\tan\beta \gtrsim 40$) can yield greater than $\mathcal{O}(1)$ contributions to R_7 even for SUSY scales of 1 TeV! Low values of $\tan\beta$ can also exhibit significant enhancements; this is demonstrated for $\tan\beta = 2$ in Fig. 5 (solid line).

Lastly, we compare the reach of rare B decays in probing SUSY parameter space with that of high energy colliders. We examine a set of five points in the minimal supergravity (SUGRA) parameter space that were chosen at Snowmass 1996 [14] for the study of supersymmetry at the NLC. Point #3 is the so-called "common" point used for a comparison of SUSY studies at the NLC, LHC, and Tev33. Once these points are chosen the sparticle mass spectrum is obtained, as usual, via the SUGRA relations and their contributions to $B \to X_s\gamma$ can be readily computed. The results are displayed in the $R_7 - R_8$ plane in Fig. 6 (labeled $1 - 5$ for each SUGRA point), along with the bounds previously obtained from our fits to the present CLEO data and to anticipated future data assuming the SM is realized. We see that four of the points should be discernable from the SM in future measurements, and that one of the points is already excluded by CLEO! We thus conclude that rare B decays are indeed complementary to high energy colliders in searching for supersymmetry.

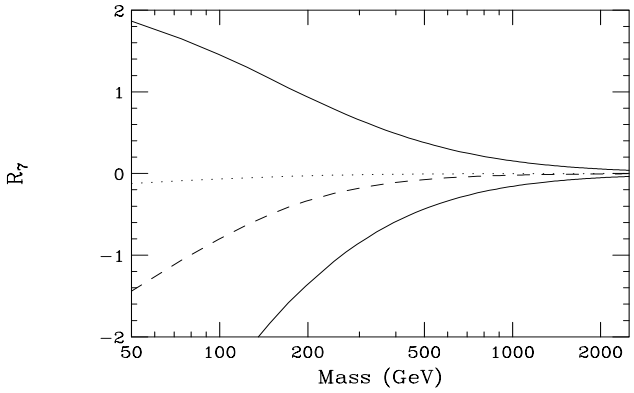

Figure 5: Contributions to R_7 in the different limits described in the text. The top solid line is the charged $H^{\pm}/t$ contribution versus $m_{H^{\pm}}$. The bottom solid line is the $\tilde{\chi}_1^{\pm}/\tilde{t}_1$ contribution versus $m_{\tilde{\chi}^{\pm}}$ where both the chargino and stop are maximally mixed states with $\mu < 0$. The dashed line is the $\tilde{H}^{\pm}/\tilde{t}_R$ contribution, and the dotted line represents the $\tilde{W}^{\pm}/\tilde{t}_1$ contribution. These two lines are both shown as a function of $\tilde{\chi}_1^{\pm}$ mass. All curves are for $\tan\beta = 2$ and $m_t = 175$ GeV.

6 Left-Right Symmetric Model in $b \to s$ Transitions

The Left-Right Symmetric Model (LRM), which is based on the extended electroweak gauge group $SU(2)_L \times SU(2)_R \times U(1)$ can lead to interesting new effects in the B system.[15,16] Due to the extended gauge structure there are both new neutral and charged gauge bosons, Z_R and W_R, as well as a right-handed gauge coupling, g_R, which is subject to the constraint $0.55 < \kappa \equiv g_R/g_L < 2.0$ from naturalness and GUT embedding conditions. After complete symmetry breaking the charged W_R mixes with the SM W_L to form the mass eigenstates $W_{1,2}$ (where W_1 is the state which is directly produced at the Tevatron and LEP II). This mixing is described by two parameters: a real mixing angle ϕ and a phase α. In most models $\tan\phi$ is naturally of order of the ratio of masses $r = M_1^2/M_2^2$, or less, in the limit of large M_2. The charged current interactions of the right-handed quarks are governed by a right-handed CKM matrix, V_R, which, in principle, need not be related to its left-handed counterpart V_L. V_R will then involve 3 new angles as well as 6 additional phases, all of which are *a priori* unknown parameters. Phenomenological constraints on the LRM are quite sensitive to variations of V_R. If one assumes manifest left-right symmetry, that is $V_R = V_L$ and $\kappa = 1$, then the $K_L - K_S$ mass difference implies that $M_R > 1.6$ TeV. However, if that assumption is relaxed and V_R (as well as κ) is allowed to vary then W_R masses as low as 500 GeV can be accomodated by

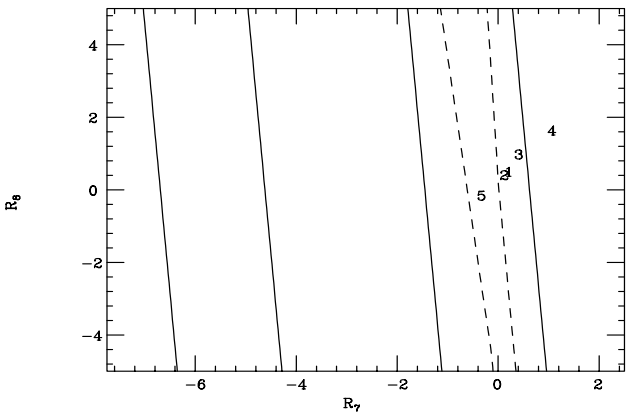

Figure 6: Values in the $R_7 - R_8$ plane for the five Snowmass NLC SUGRA points. The solid and dashed bands represent the present bounds from CLEO and those anticipated from future experiment, respectively, as described in Figure 3.

present data. This implies that the magnitude of $\tan\phi$ is $\leq few \times 10^{-2}$.

Clearly, this model contains many additional sources of CP violation. In addition, the influence of the LRM may be felt in both tree and loop-level B decays. In particular, the possibility of a large right-handed component in the hadronic current describing $b \to c$ transitions has long been a subject of discussion.[15] Here we examine the possibility of using the rare decays $B \to X_s\gamma$ and $B \to X_s\ell^+\ell^-$ as a new tool in exploring the parameter space of the LRM. The exchange of a W_R within a penguin or box diagram, in analogy with the SM W_L exchange, can lead to significant deviations from the SM predictions for the rates and kinematic distributions in these decays.

In the LRM the complete operator basis governing $b \to s$ transitions in Eq. (4) must be expanded to

$$\mathcal{H}_{eff} = \frac{-4G_F}{\sqrt{2}} \sum_{i=1}^{12} C_{iL}(\mu)\mathcal{O}_{iL}(\mu) + L \to R\,. \tag{8}$$

This includes the right-handed counterparts to the usual 10 purely left-handed operators, as well as two pairs of additional four-quark operators of mixed chirality. The 2 subsets of left- and right-handed operators, $\mathcal{O}_{1-12L,R}$ are decoupled and do not mix under REG evolution. The decay $B \to X_s\gamma$, where

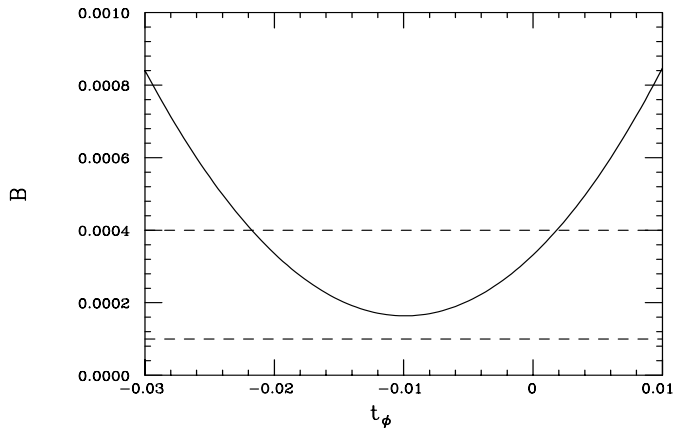

Figure 7: The $B \to X_s\gamma$ branching fraction in the LRM for $m_t(m_t) = 170$ GeV as a function of $\tan\phi$, assuming $\kappa = 1$, $V_R = V_L$, and $M_2 = 1.6$ TeV. The 95% C.L. CLEO results lie inside the dashed lines.

the operators $\mathcal{O}_{1-8,11,12(L,R)}$ contribute, has been studied in some detail.[16] In particular it was shown that the left-right mixing terms associated with $\tan\phi \neq 0$ can be enhanced by a helicity flip factor of $\sim m_t/m_b$ and can lead to significantly different predictions from the SM even when $V_L = V_R$ and W_2 is heavy. This is depicted in Fig. 7 from Rizzo.[16] It is also clear from the figure that not only is the SM result is essentially obtained when $\tan\phi = 0$, but also that a conspiratorial solution occurs when $\tan\phi \simeq -0.02$. From the $B \to X_s\gamma$ perspective, these two cases are indistinguishable, independent of any further improvements in the measurement of the branching fraction.

LRM effects in $B \to X_s\ell^+\ell^-$ have recently been examined in Ref. [17] where it is found that the observables associated with this decay can distinguish the LRM from the SM. Here, all 24 operators in Eq. (8) participate in the renormalization. The determination of the matching conditions at the electroweak scale for these 24 operators is tedious due to the large number of parameters, and in addition to new tree graphs, 116 one-loop diagrams must be evaluated. It is found that this decay can easily distinguish the LRM from the SM, even for the parameter space region which mimics the SM rate for $B \to X_s\gamma$. The extension of the operator basis in Eq. (8) implies that the conventional model independent determination of the Wilson coefficients discussed above will not apply in this case. In fact, this global fit technique has recently been shown

to fail[17] for the LRM, resulting in enormous values of $\chi^2/d.o.f.$, and hence provides a powerful probe for the existence of new operators.

7 Conclusions

This talk focused on supersymmetric and left-right symmetric model effects, as well as model independent tests for new physics, in rare B decays. Of course, there are numerous other candidates for physics models beyond the SM, as well as many other reactions where they can be tested. A brief compendium of these is given in Table 1. Here, we display the effects of (i) Multi-Higgs-Doublet Models (MHDM), with and without Natural Flavor Conservation (NFC), (ii) the Minimal Supersymmetric Standard Model (MSSM), and the supersymmetric models with squark alignment, effective SUSY scales, and R-parity violation, (iii) the LRM, with and without manifest left-right symmetry in the quark mixing matrices, (iv) a fourth generation, and (v) models with Z-boson mediated FCNC. We describe whether these models have the potential to cause large deviations from SM predictions in rare decays and $D^0 - \bar{D}^0$ mixing, whether new phases exist which contribute to $B_d^0 - \bar{B}_d^0$ mixing, and whether the new physics effects cancel in the ratio of mass differences in the B_s to B_d systems. This table is only intended to give a quick indication of potential effects.

In conclusion, we see that the B sector can provide a powerful probe, not only for the existence, but also for the structure of physics beyond the SM.

1. See, for example, P. Huet and E. Sather, *Phys. Rev.* **D51**, 379 (1995).
2. G. Barenboim, G. Eyal, and Y. Nir *Phys. Rev. Lett.* **83**, 4486 (1999).
3. CDF Collaboration, T. Affolder *et al.*, hep-ex/9909003.
4. CLEO Collaboration, S. Ahmed *et al.*, hep-ex/9908022; CLEO Collaboration, M.S. Alam *et al.*, *Phys. Rev. Lett.* **74**, 2885 (1995); CLEO Collaboration, R. Ammar *et al.*, *Phys. Rev. Lett.* **71**, 674 (1993); ALEPH Collaboration, R. Barate *et al.*, *Phys. Lett.* **B429**, 169 (1998).
5. M. Misiak, these proceedings; T. Morozumi, these proceedings.
6. T. Inami and C.S. Lim, Prog. Theor. Phys. **65**, 297 (1981).
7. A.J. Buras and M. Münz, *Phys. Rev.* **D52**, 186 (1995).
8. A. Ali *et al.*, *Phys. Rev.* **D61**, 074024 (2000); G. Buchalla and G. Isidori, *Nucl. Phys.* **B525**, 42 (1998).
9. A. Czarnecki and W. Marciano, *Phys. Rev. Lett.* **81**, 277 (1998).
10. A. Kagan and M. Neubert, Eur. Phys. J **C7**,5 (1999).
11. A. Ali, T. Mannel, and T. Morozumi, *Phys. Lett.* **B273**, 505 (1991); A. Ali, G. F. Giudice, and T. Mannel, *Z. Phys.* **C67**, 417 (1995).
12. J.L. Hewett, *Phys. Rev.* **D53**, 4964 (1996).

Model	Rare Decays	$\frac{\Delta M_s}{\Delta M_d}$	New Phase B_d Mixing	$D^0 - \bar{D}^0$ Mixing
MHDM: with NFC	$B \to X_s\gamma$	= SM	No	Small
: no NFC	Not Really	$\neq$ SM	Yes	Big
MSSM	$B \to X_s\gamma$	= SM	No	Small
Squark Alignment	Small	$\sim$ SM	No	Huge
Effective SUSY	Small	$\sim$ SM	Yes	Small
R-Parity Violation	Big	$\neq$ SM	Yes	Big
LRM: $V_L = V_R$	$B \to X_s\gamma$ and	= SM	No	Small
: $V_L \neq V_R$	$B \to X_s\ell^+\ell^-$	$\neq$ SM	Yes	Big
4th Generation	Big	$\neq$ SM	Yes	Huge
Z-mediated FCNC	Big	$\neq$ SM	Yes	Big

Table 1: Model dependent effects of new physics in various processes.

13. J.L. Hewett and J.D. Wells, *Phys. Rev.* **D55**, 5549 (1997), and references therein.
14. M.N. Danielson *et al.*, Proceedings of *New Directions for High-Energy Physics*, Snowmass, CO, 1996, ed. D.G. Cassel *et al.*.
15. M.B. Voloshin, hep-ph/9704278; M. Gronau and S. Wakaizumi, *Phys. Rev. Lett.* **68**, 1814 (1992); T.G. Rizzo, *Phys. Rev.* **D58**, 055009 (1998); W. Goldberger, hep-ph/9902311.
16. D. Cocolicchio *et al.*, *Phys. Rev.* **D40**, 1477 (1989); G.M. Asatryan and A.N. Ioannisyan, Yad. Fiz. **51**, 1350 (1990); K.S. Babu, K. Fujikawa, and A. Yamada, *Phys. Lett.* **B333**, 196 (1994); P. Cho and M. Misiak, *Phys. Rev.* **D49**, 5894 (1994); T.G. Rizzo, *Phys. Rev.* **D50**, 3303 (1994); G. Bhattacharyya and A. Raychaudhuri, *Phys. Lett.* **B357**, 119 (1995); T.G. Rizzo, hep-ph/9705209.
17. T.G. Rizzo, *Phys. Rev.* **D58**, 114014 (1998); S. Fukae, C.S. Kim, T. Morozumi, and T. Yoshikawa, *Phys. Rev.* **D59**, 074013 (1999); S. Fukae, C.S. Kim, and T. Yoshikawa, hep-ph/0003053.